TECHNISCHE HOCHSCHULE DEGGENDORF

MASTER THESIS

Structured generation of correlations in the objective function by varying the ansatz in VQAs

---

Author:
Muhammad Shahzaib
12305029

Supervisors:
Prof. Dr. Helena Liebelt
Tobias Bauer(LRZ)

A thesis submitted in fulfillment of the requirements
for the degree of Masters

in the

High Performance Computing/Quantum Computing
Fakultät Angewandte Informatik

Deggendorf, January 31, 2025

Declaration of Authorship

Name of student: Muhammad Shahzaib
Name of supervisor: Prof. Dr. Helena Liebelt, Tobias Bauer
Thesis topic: Structured generation of correlations in the objective function by varying the ansatz in VQAs

I hereby declare that the thesis has been written in compliance with Section 35 (7) RaPO (State Examination Regulations in Bavaria BayRS 2210-4-1-4-1-WFK), is my own work, has not been submitted for any other degree at any other university or institution, does not contain or use any sources or resources other than those referenced, and that all direct and paraphrased quotes have been duly cited as such.

Deggendorf, 31.01.2025
(Date)

(Signature of student)

TECHNISCHE HOCHSCHULE DEGGENDORF

Abstract

High Performance Computing/Quantum Computing
Fakultät Angewandte Informatik

Masters

Structured generation of correlations in the objective function by varying the ansatz in VQAs

by Muhammad Shahzaib

This thesis investigates the impact of ansatz design on the performance of Variational Quantum Algorithms (VQAs) in solving diverse problem Hamiltonians. Specifically, it compares the effectiveness of the Generic Ansatz and the QAOA Ansatz in approximating ground states for three distinct problem types: the electronic structure of lithium hydride (LiH), the MaxCut optimization problem for a complete graph of 12 nodes, and the Transverse-Field Ising Model (TFIM) in two different configurations. A modified version of the Generic Ansatz was also tested against these TFIM configurations to evaluate the interplay between ansatz structure and problem composition. A consistent classical optimizer, COBYLA, was used throughout the work to isolate the impact of ansatz structures on algorithm performance. The results demonstrated that the Generic Ansatz consistently converged closer to the exact ground states across all problem types, outperforming the QAOA ansatz. This was particularly evident in the MaxCut problem, where the Generic Ansatz outmatched the QAOA Ansatz despite the latter being specifically designed for combinatorial optimization tasks. To ensure a fair comparison, the number of layers for both ansätze was restricted to one. While increasing the number of QAOA layers could improve its performance, it would also raise computational costs. Additionally, when the form of Generic Ansatz was adjusted to align with the TFIM configuration, it yielded improved results. By revealing the strengths and limitations of different ansatz structure, this work aims to advance the understanding of how ansatz design correlates with the given objective function, and in turn, influences the success of quantum algorithms.

Acknowledgements

First and foremost, I would like to express my deepest gratitude to my professor and supervisor, Prof. Dr. Helena Liebelt for her invaluable guidance, unwavering support and insightful feedback throughout this journey. Her expertise and encouragement have been instrumental in shaping me as a researcher.

I am also sincerely thankful to my supervisor at Leibniz-Rechenzentrum, Tobias Bauer, for generously providing his expertise and knowledge. His constructive feedback and constant help throughout the course of this research have been invaluable and greatly appreciated. Also, many thanks to Dr. Luigi Iapichino for lending his deep knowledge and research expertise, as well as for his guidance and support throughout this project.

This research would not have been possible without the foundational idea and guidance provided by Amit J. Gangapuram. His insights and initial contributions served as a critical starting point for this work, shaping its direction and enabling further exploration.

I am deeply grateful to my colleagues and classmates for providing a space to brainstorm ideas and helping me navigate the challenges on this tricky road. I am also thankful to my family and friends for helping proofread the thesis and being patient with me during this time.

Lastly, I extend my gratitude to everyone who has supported me, directly or indirectly, during this journey; your contributions have made this work possible.

Contents

Declaration of Authorship iii

Abstract v

1 Introduction 1

2 Background 3
  2.1 Variational Quantum Algorithms 3
    2.1.1 Objective Function 4
    2.1.2 Ansatz 4
    2.1.3 Optimizer 5

3 Methods 9
  3.1 Problem Hamiltonian 9
    3.1.1 Molecular Hamiltonian 9
    3.1.2 MaxCut Problem 12
    3.1.3 Transverse-Field Ising Model 14
  3.2 Ansatz 15
    3.2.1 Generic Ansatz 15
    3.2.2 QAOA Ansatz 18

4 Results 19
  4.1 Ground State of LiH 19
  4.2 MaxCut Problem on a K-12 Graph 22
  4.3 Solving the Transverse-Field Ising Model 23

5 Conclusion & Outlook 29

A Supplementary Material 31
  A.1 Software, Libraries and System Specs 31
    A.1.1 Hardware 31
    A.1.2 Software 31
  A.2 Code Implementation 31

Bibliography 33

List of Figures

2.1 VQA Process 4
2.2 Energy landscape for theta 7
2.3 Energy landscape for beta and gamma 7

3.1 K4 Graph 13
3.2 Generic Ansatz 16
3.3 Generic Ansatz without the last CNOT 17
3.4 QAOA Ansatz 17

4.1 LiH with Generic Ansatz 20
4.2 LiH with QAOA Ansatz 21
4.3 K-12 graph 22
4.4 MaxCut with Generic Ansatz 23
4.5 MaxCut with QAOA Ansatz 24
4.6 TFIM chain with Generic Ansatz 25
4.7 TFIM chain with Generic Ansatz without the last CNOT . . . 25
4.8 TFIM circular with Generic Ansatz 26
4.9 TFIM circular with Generic Ansatz without the last CNOT . . 26
4.10 TFIM chain with QAOA Ansatz 27
4.11 TFIM circular with QAOA Ansatz 28

Chapter 1

Introduction

Quantum computing is an emerging field with the potential to solve computational problems that are intractable for classical computers (Preskill, 2018; Arute, Arya, Babbush, et al., 2019). Among the most promising of these quantum algorithms are Shor's algorithm, which promises an exponential speedup for factoring large integers and solving discrete logarithms (Shor, 1997), and Quantum Phase Estimation (QPE), which offers a powerful approach for solving large eigenvalue problems (Cao et al., 2019). QPE seeks to make advancements in the fields of quantum chemistry and materials science, while also serving as a foundational building block for algorithms like Shor's. However, both of these algorithms require large-scale fault-tolerant quantum computers that are still out of reach. The next significant strategy is to employ the Variational Quantum Algorithms (VQAs) which combine quantum circuits with classical optimization to solve problems but on a smaller scale. VQAs are particularly suitable for Noisy Intermediate-Scale Quantum (NISQ) devices because they are expected to leverage the current noisy devices due to their hybrid quantum-classical nature which allows them to work well even in the presence of noise and imperfections. At the heart of VQAs is the ansatz, a parameterized quantum circuit, and its pairing with the objective Hamiltonian. However, the ability of a particular ansatz to approximate the ground state of a given Hamiltonian is an area of ongoing investigation.

This thesis investigates how different ansätze perform when applied to specific Hamiltonians. Given an ansatz $A(\theta)$ and an objective Hamiltonian H, how well does $A(\theta)$ generate the correlations of the ground state of H given by the expectation value of H as $\langle \psi(\vec{\theta}) | H | \psi(\vec{\theta}) \rangle$. The key idea is to understand the capability of a given ansatz to generate the required correlations in the ground state of the target Hamiltonian. The study focuses on two ansätze: the Generic Ansatz, which is broadly applicable to various problems, and the Quantum Alternating Operator Ansatz or QAOA Ansatz, which is specifically tailored for combinatorial optimization problems. Their performance is assessed on three distinct problems: the electronic structure calculation of lithium hydride (LiH), the MaxCut combinatorial optimization problem of a complete graph of 12 vertices, and the Transverse-Field Ising Model (TFIM).

A key assumption in the analysis is that the classical element of VQAs, the optimizer, does not significantly affect the convergence of the algorithm. The optimizer is set to COBYLA throughout the process to maintain the optimization consistent and isolate the ansatz performance. This allows to contribute the measured differences in the performance and accuracy of the results to the ansatz rather than the optimization techniques used.

The motivation for this study comes from the need to understand which ansätze are effective on a range of problems, and if the structure of an ansatz plays a significant role in the convergence of a given problem. While QAOA is catered towards the optimization problems, the Generic Ansatz offers a more basic and general structure which is applicable to a number of problems. By rigorously testing the performance of these ansätze across multiple computational tasks, this thesis seeks to highlight the impact of the choice of ansatz on its ability to find the ground state of the problem Hamiltonians.

The insights gained from this work aim to contribute to the ongoing development of the quantum algorithms by identifying the relative strengths and limitations of the ansätze considered in this study. This study is an exercise in trying to understand the critical interplay between the ansatz structure and the anatomy of a problem Hamiltonian. This knowledge is instrumental in allowing to make informed decisions when it comes to ansatz selection for particular problem sets.

The thesis is structured as follows: Chapter 2 describes the workflow of the Variational Quantum Algorithms (VQAs) and delves into the individual parts of the process. Chapter 3 details all the methodology used in the work as in the different problem Hamiltonians which form the basis of this study alongside the ansätze used against those Hamiltonians to research the effectiveness of said ansätze. In Chapter 4, the results of the research about the performance and accuracy of the ansätze is presented along with a comprehensive analysis of said results. Chapter 5 discusses the broader implications of the results, the limitations of the method, and suggests directions for future research.

Chapter 2

Background

2.1 Variational Quantum Algorithms

As discussed above, VQAs are a class of hybrid quantum algorithms that harness the power of quantum and classical computation side by side to perform various computational tasks. These algorithms are specially geared towards the **N**oisy **I**ntermediate-**S**cale **Q**uantum Computers (NISQ) because they work well with the limited number and quality of qubits available nowadays. VQAs achieve this by employing shallower parameterized quantum circuits and outsourcing the optimization to classical techniques, as opposed to other quantum algorithms like quantum phase estimation which require increased depth and highly coherent qubits (Reiher et al., 2017) to perform similar tasks.

At the center of this process (shown in Fig. 2.1) is a parameterized circuit characterized by unitaries with varying angles, known as *ansatz*, $|\psi(\vec{\theta})\rangle$ with some adjustable parameter $\vec{\theta}$. These parameters vary according to the problem but usually represent the degree by which a quantum gate rotates in the circuit. The process begins with a guess value for these angles, say θ_0, to prepare a quantum state $|\psi(\vec{\theta_0})\rangle$. The *objective function* is some function of the parameterized quantum state, here the expectation value, obtained by the action of the parameterized unitaries as follows:

$$C(\vec{\theta}) = \langle\psi(\vec{\theta})|H|\psi(\vec{\theta})\rangle \tag{2.1}$$

where the $C(\vec{\theta})$ is the objective function, also called cost function, which is equal to the expectation value of a problem-specific Hamiltonian H with respect to the parameterized quantum state. This objective value is then passed to a classical *optimizer* that updates the given parameter accordingly. These updated parameters are then used to reconstruct the parameterized quantum state and this feedback process is looped until a desired convergence is

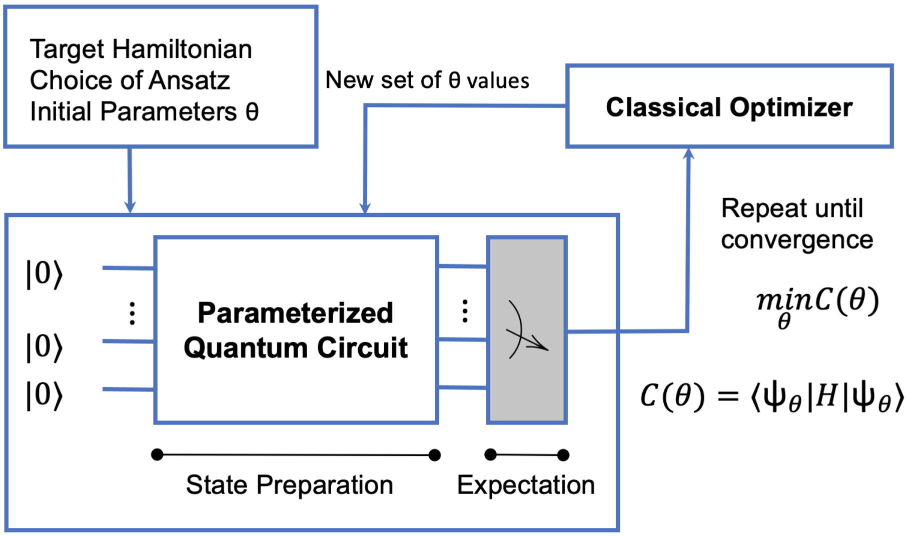
Target Hamiltonian
Choice of Ansatz
Initial Parameters θ
New set of θ values
Classical Optimizer
Repeat until convergence
$\min_\theta C(\theta)$
$|0\rangle$
$|0\rangle$
$|0\rangle$
Parameterized Quantum Circuit
$C(\theta) = \langle\psi_\theta|H|\psi_\theta\rangle$
State Preparation
Expectation

FIGURE 2.1: Graphical representation of Variational Quantum Algorithm process

achieved. The details of each of the components of VQAs will be discussed in the following.

2.1.1 Objective Function

In VQAs, the importance of the cost function lies in guiding the optimization process. It serves as a measure of the performance of the VQA, that is, how close a converged result is to the desired value. As seen in Eq. 2.1, the problem to be solved is encoded in the function; and the result is an expectation value of some operator, in our case, H. For example, in the case of quantum chemistry problems, the objective function calculates the expectation value of a molecular Hamiltonian, resulting in the energy of the said molecular system. Moreover, the cost function essentially provides a hyper-curve which the optimizer then navigates to bring us to the maxima or minima (Cerezo, Arrasmith, Babbush, et al., 2021).

2.1.2 Ansatz

The concept of ansatz, or an initial guess state, comes from the variational principle in quantum mechanics. The variational principle is used to estimate the ground state of a system described by the Hamiltonian H with respect to some initial "trial" function ψ. In this sense, this initial "trial" function is called the ansatz of our system. The variational principle says:

$$E_g \leq \langle \psi | H | \psi \rangle \equiv \langle H \rangle \tag{2.2}$$

This means that the expectation value of an unknown system Hamiltonian H with any normalized function ψ will be an upper bound of the ground state energy E_g. This also implies that the more accurate initial guess function will land closer to the approximation of the ground state. The proof of this principle is given in Griffiths and Schroeter, 2020.

In the context of Variational Quantum Algorithms (VQAs), an ansatz refers to a parameterized unitary operator, typically represented as a quantum circuit. The ansatz defines a family of quantum states that can be adjusted through its parameters to approximate the solution of the problem described by the Hamiltonian. Its design determines how efficiently the algorithm explores the solution space, balancing expressivity, the ability to represent a wide range of solutions, and trainability, the ability to converge to an optimal solution without encountering issues like local minima. Depending on its structure, the ansatz may either facilitate effective optimization or hinder the process by introducing excessive complexity or irrelevant subspaces. Further details on the types of ansätze explored in this research, along with their performance and selection criteria, will be provided in section 3.

2.1.3 Optimizer

Optimizers are the classical component of the VQAs, responsible for iteratively fine-tuning the parameters of the objective function until a convergence is reached. However, the optimization landscape of these problems can be challenging due to several factors. One such problem is the presence of local minima in the optimization landscape, also referred to as barren plateau in the context of VQAs. A barren plateau is a region in the parameter landscape where the cost function gradient becomes exponentially small with respect to the increasing qubit number, making it hard to optimize the parameters. This typically occurs due to the exponential growth of the Hilbert space, causing the cost landscape to become flat and uninformative. McClean et al., 2018 delves deeper into this problem, explaining the difficulty of optimization in such cases. Fig. 2.2 illustrates a relatively smooth and convex energy landscape as a function of one parameter, but the problem exacerbates moving into higher dimensional parameter spaces. Adding only one more parameter to the same problem results in the plot shown in Fig. 2.3, showing several local minima. As a result, optimizers may converge prematurely to suboptimal solutions, failing to identify the right global minimum.

Another challenge is that the optimization task for VQAs is generally an NP-hard problem (Bittel and Kliesch, 2021). This implies that the classical part of the workflow might take more time than the quantum processing. Consequently, optimizers play a crucial role in determining the efficiency and success of the VQA procedure. Factors such as the optimizer's ability to escape local minima and adapt to barren plateaus significantly influence the performance of the algorithm.

Two important settings for the optimizer are `maxiter` and `tol`, which influence how the optimization proceeds. The parameter `maxiter` defines the maximum number of iterations the optimizer is allowed to perform before rendering the optimization unsuccesful, which in this study was set to 500 to balance computational cost with the ability to explore the parameter landscape. The `tol` parameter specifies the convergence threshold for the optimization, with smaller values requiring higher precision. A `tol` value of 10^{-6} was used to ensure the optimizer terminated only when a highly precise solution was found.

Random initialization of parameters was employed for each optimization run. This approach introduces diversity in starting points, which is important in overcoming barren plateaus or local minima. However, it also results in variability in the outcomes of the runs, as different initial parameters can lead to convergence to different regions of the cost landscape. The clustering of results observed in this study reflects the optimizer's tendency to settle near slopes or local minima, influenced by both the choice of ansatz and the cost landscape itself. These results are presented in the Chapter 4.

The main focus of the study was exploring the effects of varying the ansatz against different problem Hamiltonians, while the optimizer, COBYLA, was kept constant throughout the process. This decision was made to isolate and analyze the impact of quantum components of the algorithm, ensuring that variations in performance could be attributed to changes in ansatz and Hamiltonian rather than the choice of optimizer. However, it is acknowledged that using different optimization techniques could offer additional insights about the performance of VQAs.

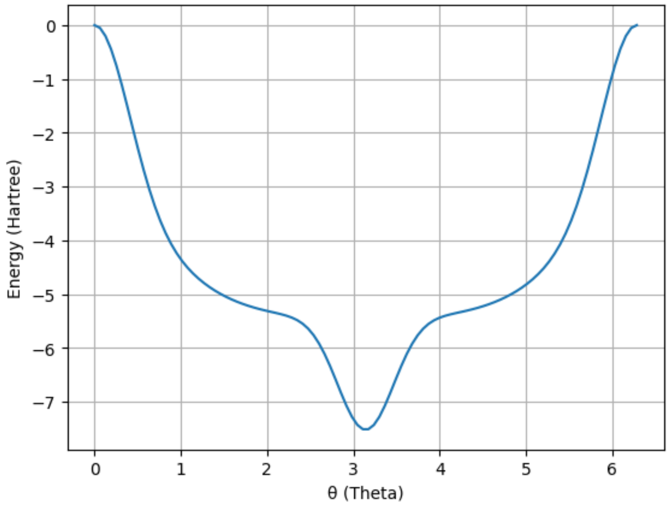

FIGURE 2.2: Energy landscape of LiH molecule as a function of θ showing the variation in the energy as the parameter sweep through 0 to 2π

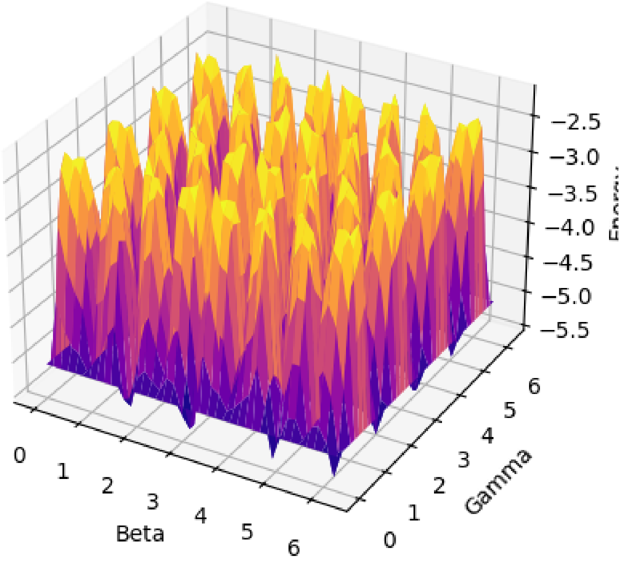

FIGURE 2.3: Energy landscape of LiH molecule as a function of β and γ showing the variation in the energy as the parameters sweep through 0 to 2π

Chapter 3

Methods

This chapter explores the research methodology, building on the topics discussed briefly in Chapter 2. It begins with the examination of the problem Hamiltonians that form the foundation of this study. With each changing Hamiltonian H, results in a new objective function (Eq. 2.1) to minimize. These Hamiltonians, which encode the physical systems and computational problems to be examined, are described in terms of their structure, significance, and relevance to the VQAs. Following that, the details of the ansätze used in this process are presented, along with their mathematical formulation, circuit design, and the rationale for their selection.

3.1 Problem Hamiltonian

As discussed above, in Variational Quantum Algorithms (VQAs), the problem Hamiltonian represents the mathematical formulation of a system or a problem to be solved. This Hamiltonian, denoted by H, encodes the energy landscape of the objective function, where the goal is to find such a configuration that optimizes the said Hamiltonian. Three different families of problems were considered for this study, which will be discussed in detail below.

3.1.1 Molecular Hamiltonian

Understanding the ground state of molecules is central to quantum chemistry and material science. The ground state of a molecule corresponds to the most stable configuration of a molecule and is crucial for predicting the chemical reactions and studying the molecular structures and material properties. The work was based on the Variational Quantum Eigensolver (VQE), (Peruzzo, McClean, Shadbolt, et al., 2014) which is a quantum-classical algorithm used to calculate the ground state energies of quantum systems, mostly molecular system. (Fedorov, Peng, Govind, et al., 2022)

To get the molecular Hamiltonian, the first principles (i.e., already established laws of physics like the mass of the electron, the charge of particles, and the Columbic forces), or also called *ab initio method*, are used to calculate the electronic structure of molecules using Schrödinger's equation. The molecular Hamiltonian is a quantum mechanical operator that describes the total energy of a molecule, encompassing the kinetic energy and the potential energy arising from the attractive and repulsive forces of the system defined in terms of the spatial geometry of the molecule and the distance of each particle (electrons and nuclei) to the other. From this information, the task is to find the electronic wavefunction that corresponds to the lowest energy state, the ground state. The sum of all the kinetic and potential energies of the molecule is given by:

$$\hat{H} = \hat{T}_e + \hat{T}_n + \hat{V}_{ee} + \hat{V}_{en} + \hat{V}_{nn} \tag{3.1}$$

where $\hat{H}$ is the Hamiltonian representing the total energy of the system. $\hat{T}_e$ is the kinetic energy of the electrons. $\hat{T}_n$ is the kinetic energy of the nuclei. $\hat{V}_{ee}$ represents the electron-electron repulsive energy. $\hat{V}_{en}$ gives us the attractive nuclei-electron energy. $\hat{V}_{nn}$ represents the nuclei-nuclei repulsion.

Equation 3.1 was simplified using the Born-Oppenheimer approximation (Born and Oppenheimer, 1927). It states that for a moving electron, a relatively heavy nucleus can be considered stationary, so $\hat{T}_n$ can be completely ignored. The term $\hat{V}_{nn}$, which depends on the relative distance of the nuclei, is treated as a constant since the nuclei are stationary. Following, the individual terms of 3.1 are explained, starting with the operator for the kinetic energy of the electrons.

$$\hat{T}_e = -\frac{\hbar^2}{2m_e}\sum_i \nabla_i^2 \tag{3.2}$$

Where $\hbar$ is the reduced Planck's constant ($\hbar = h/2\pi$), m_e is the mass of an electron, and ∇_i^2 is the Laplacian for the i-th electron.

$$\hat{V}_{ee} = \sum_{i<j} \frac{e^2}{4\pi\varepsilon_0|\mathbf{r}_i - \mathbf{r}_j|} \tag{3.3}$$

$|\mathbf{r}_i - \mathbf{r}_j|$ is the distance between the i-th and j-th electrons. ε_0 is the constant of permittivity of free space.

$$\hat{V}_{en} = -\sum_{i,I} \frac{Z_I e^2}{4\pi\varepsilon_0 |\mathbf{r}_i - \mathbf{R}_I|} \tag{3.4}$$

Z_I is the charge of nucleus I in terms of e and $|\mathbf{r}_i - \mathbf{R}_I|$ is the distance between the i-th electron and nucleus I.

This further provides the simplified electronic Hamiltonian after the Born-Oppenheimer approximation as:

$$\hat{H}_{\text{elec}} = -\frac{\hbar^2}{2m_e} \sum_i \nabla_i^2 - \sum_{i,I} \frac{Z_I e^2}{4\pi\varepsilon_0 |\mathbf{r}_i - \mathbf{R}_I|} + \sum_{i<j} \frac{e^2}{4\pi\varepsilon_0 |\mathbf{r}_i - \mathbf{r}_j|} \tag{3.5}$$

The next task is to encode this Hamiltonian in a way that quantum computers can work with. The discussion of the quantum chemistry aspect of the process is kept consise. For a more comprehensive overview, refer to Tilly et al., 2022. The coordinates of the atoms in the molecule are given to PySCFDriver, which is an interface between quantum chemistry methods (PySCF (Python for Quantum Chemistry)) and quantum algorithms, providing a convenient way to run electronic structure calculations and feeding the results to the quantum algorithms. The molecular coordinates are in the form `Li 0 0 0; H 0 0 1.5949`, meaning the lithium atom is considered to be at the origin of the Cartesian coordinates and the hydrogen atom is away 1.5949 angstroms in the z direction.

In the following, the one-electron and two-electron integrals are shown which are crucial for mapping the molecular Hamiltonians to quantum circuits. They are needed for expressing the Hamiltonian in terms of fermionic creation and annihilation operators ($\hat{a}_p^\dagger, \hat{a}_q$) which can be mapped into strings of Pauli gates using the Jordan-Wigner mapping.

$$h_{pq} = \int \phi_p^*(\mathbf{r}) \left(-\frac{\hbar^2}{2m} \nabla^2 - \sum_I \frac{Z_I e^2}{4\pi\varepsilon_0 |\mathbf{r} - \mathbf{R}_I|} \right) \phi_q(\mathbf{r}) \, d\mathbf{r} \tag{3.6}$$

The one-electron integral includes the kinetic energy of electrons and the electron-nucleus attraction energy.

$$h_{pqrs} = \int \int \phi_p^*(\mathbf{r}_1) \phi_q(\mathbf{r}_1) \frac{e^2}{4\pi\varepsilon_0 |\mathbf{r}_1 - \mathbf{r}_2|} \phi_r^*(\mathbf{r}_2) \phi_s(\mathbf{r}_2) \, d\mathbf{r}_1 d\mathbf{r}_2 \tag{3.7}$$

The two-electron integral includes the electron-electron potential energy.

$$\hat{H} = \sum_{pq} h_{pq} \hat{a}_p^\dagger \hat{a}_q + \frac{1}{2} \sum_{pqrs} h_{pqrs} \hat{a}_p^\dagger \hat{a}_q^\dagger \hat{a}_r \hat{a}_s \tag{3.8}$$

The final Hamiltonian is now in second quantization in terms of creation and annihilation operators $\hat{a}_p^\dagger, \hat{a}_q$. Which can be directly translated to strings of Pauli-gates: I, X, Y, Z by the Jordan-Wigner transformation and thus can be simulated on a quantum computer.

$$\hat{a}_p^\dagger \rightarrow \frac{1}{2}\left(X_p - iY_p\right) \bigotimes_{j=0}^{p-1} Z_j \tag{3.9}$$

$$\hat{a}_p \rightarrow \frac{1}{2}\left(X_p + iY_p\right) \bigotimes_{j=0}^{p-1} Z_j \tag{3.10}$$

The final Hamiltonian can be shown in the form of Pauli strings as:

$$\hat{H} = \sum_i c_i P_i \tag{3.11}$$

where P_i are tensor products of Pauli matrices (e.g., $X \otimes Y \otimes Z \otimes I$).

The problem Hamiltonian in this case was chosen as lithium hydride (LiH) because of its relatively small number of electrons and well-understood spatial data. The minimal basis-set STO-3G was used to map the molecule to the qubits. It is an approximation of the Slater-type orbital (STO) functions commonly used in quantum chemistry for molecular simulations. The STO-3G basis set represents each atomic orbital as a linear combination of three Gaussian functions, which simplifies the mathematical representation while keeping the electronic properties of the molecule. In the case of LiH, the STO-3G mapping results in 12-qubit representation of the Hamiltonian, making it feasible to run on simulated quantum environments.

3.1.2 MaxCut Problem

The MaxCut problem is a well-known combinatorial optimization problem in the field of graph theory. It is an NP-hard problem and has applications in network design and circuit partitioning, among others.

Given a graph $G = (V, E)$ where V is the set of vertices (or nodes) of the graph and E is the set of the edges (or links) between those vertices in V; the goal of the MaxCut problem is to divide the vertices of the graph into two subsets such that the number of edges cut is maximized. For example, for a complete graph, also called K-4 graph shown in 3.1, $V = \{0, 1, 2, 3\}$ and $E = \{(0,1), (0,2), (0,3), (1,2), (1,3), (2,3)\}$. A cut divides the vertices into two subsets S and T such that $S \subset V, \quad T = V \setminus S$. An edge is "cut" if

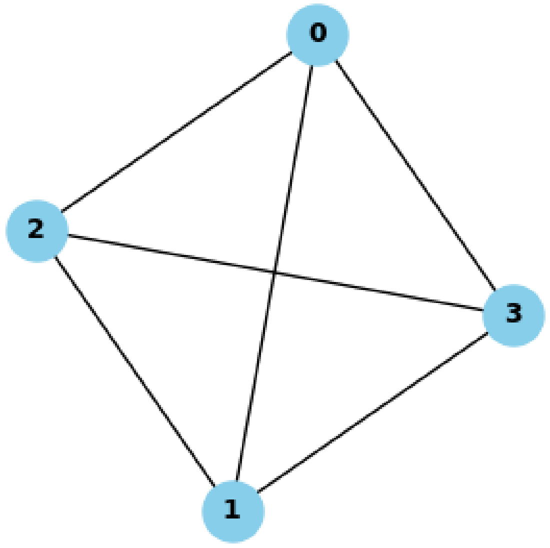

FIGURE 3.1: A complete graph with four vertices and six edges

it connects a vertex from S to T. In our example, consider $S = \{0, 1\}$ and $T = \{2, 3\}$, dividing the vertices in these two subsets. The number of edges which connect the vertices from S to T are four: $(0, 2), (0, 3), (1, 2), (1, 3)$, so, the maximum number of edges cut is four in this case.

For each vertex $i \in V$, a binary variable $x_i \in \{0, 1\}$ is assigned indicating which subset the vertex belongs to. For each edge (u, v) in the graph G:

$$C_{(u,v)}(x) = x_u + x_v - 2x_u x_v \tag{3.12}$$

$C_{(u,v)}(x) = 1$ if the edge is cut, otherwise the function equals 0. The goal is to maximize the following objective function of the whole problem.

$$C_{(u,v)}(x) = \sum_{(u,v)\in E} x_u + x_v - 2x_u x_v \tag{3.13}$$

To encode this problem into a form quantum computers can work with, each vertex is mapped to one qubit. And each qubit can be in the state $|0\rangle$ or $|1\rangle$ depending on which subset S or T it belongs to. Since σ_z, the Pauli-Z gate, also has the same eigenstates with eigenvalues 1 and -1, $\sigma_z|0\rangle = |0\rangle$ and $\sigma_z|1\rangle = -|1\rangle$, it can be used to encode the problem. Since,

$$f(x) = \frac{x+1}{2} = \begin{cases} 0 & \text{if } x = -1, \\ 1 & \text{if } x = 1. \end{cases}$$

the x in Eq. 3.13 can be replaced with $\frac{\sigma_z+I}{2}$, where I is the identity matrix, to get this Hamiltonian:

$$H_{MaxCut} = \sum_{(u,v)\in E} \frac{\sigma_z^u + I}{2} + \frac{\sigma_z^v + I}{2} - 2(\frac{\sigma_z^u + I}{2})(\frac{\sigma_z^v + I}{2}) \tag{3.14}$$

This Hamiltonian is simplified as shown below:

$$H_{MaxCut} = \sum_{(u,v)\in E} \frac{I - \sigma_z^u \sigma_z^v}{2} \tag{3.15}$$

To align with the task of minimizing the Hamiltonian energy, Eq. 3.15 is multiplied by -1 for each cut made. As a result, minimizing the Hamiltonian energy corresponds to the maximum number of edges cut. For a more detailed analysis, see Wang et al., 2018 and Shusen Liu, 2022.

3.1.3 Transverse-Field Ising Model

The transverse-field Ising model as given in Fradkin, 2013 describes a system of spin projections, a quantum version of the Ising model, with interactions along the z axis and an external magnetic field along the x axis. Since the spin projections along the perpendicular axis do not commute, i.e., they cannot be observed simultaneously, the model requires analysis within the framework of quantum mechanics. The slightly modified version of that Hamiltonian is:

$$H_{\text{TFIM}} = -\sum_{i=1}^{N-1} \sigma_z^i \sigma_z^{i+1} - g\sum_{i=1}^{N} \sigma_x^i \tag{3.16}$$

Where N is the number of qubits/spins in the chain, σ_z and σ_x are the Pauli-Z and X gates respectively, and g is the strength of the transverse field. The first term in the Hamiltonian describes the nearest-neighbor interaction throughout the chain; while the second term represents the transverse magnetic field applied to each qubit. The quantum effect in this model arises from this second term in the Hamiltonian since the eigenvectors of σ_x, $\frac{1}{\sqrt{2}}(|0\rangle \pm |1\rangle)$, push the ground state of the Hamiltonian towards the superposition state. The stronger the magnetic field strength, the stronger the superposition in the ground state. In extreme cases:

- $g \to 0$, in this case, the transverse field term becomes negligible, and the model behaves as the classical Ising model, and tends towards the *ordered phase*. The qubits interact with each other in a *ferromagnetic* way and all of the spins align toward $|0\rangle$ or $|1\rangle$, giving us the ground state of form $|000\ldots0\rangle$ or $|111\ldots1\rangle$.

- $g \to \infty$, in this limit, the transverse field term dominates, which leads to qubits in superposition states all over the system giving us a highly superposed state in the Z-basis but a product state in the X-basis. This phase is referred to as *disordered phase*.

The balance between the interaction term and the transverse field term governs the quantum behavior of the system. And at a critical value of g, there is a *quantum phase transition* between these two regimes.

To test the interplay between the ansatz and the Hamiltonians, another form of 3.16 was used, where instead of a straight chain-like interaction between each successive qubit, a connection between the first qubit and the last qubit is added as shown in Fig. 3.3.

3.2 Ansatz

This section introduces the ansätze used in this work, outlining their structure, parameterization, and their ability to represent the quantum states required for solving the target problems. Each ansatz has unique features and advantages, tailored to the demands of specific Hamiltonians fulfilling the task to study the correlations between the objective functions with different ansätze. As discussed in Chapter 2, the choice of ansatz plays a crucial role in determining the effectiveness and the complexity of the optimization. In the following, the theoretical foundations and practical implementations of the Generic Ansatz and QAOA Ansatz are presented in detail.

3.2.1 Generic Ansatz

The Generic Ansatz, illustrated in Fig. 3.2, is inspired by the Basic Entangler circuit introduced by PennyLane, 2024. As the name suggests, it is a simple yet effective parameterized quantum circuit. It consists of two distinct layers. The first layer L_1 consists of R_y rotation gates applied to each qubit, where the angles θ_i serve as tunable parameters. These parameters are central to the optimization process, as they are the only tunable part of the circuit, and also provide the circuit with the flexibility to explore the solution space. Mathematically, this layer is represented as $L_1 = \prod_{i=1}^{n} R_Y(\theta_i)$, where n is the number of qubits in the circuit.

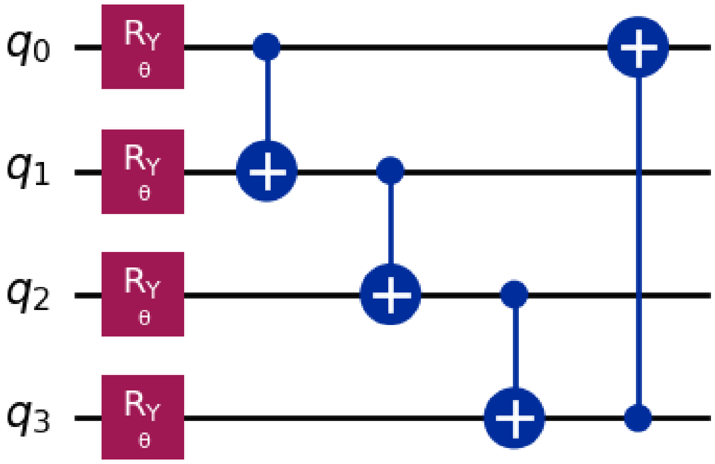

FIGURE 3.2: Generic Ansatz: Y-rotation gates followed by circular CNOT gates

The second layer L_2 is composed of CNOT gates that entangle the qubits. These qubits are arranged so that each qubit is connected to its next neighbor, with an additional CNOT gate linking the last qubit to the first. This arrangement is referred to as circular entanglement and adds to the expressiveness of the circuit by allowing a non-local interaction. The structure of this layer is expressed as $L_2 = \prod_{i=1}^{n} CNOT_{i+1}^{i} \cdot CNOT_{1}^{n}$. While the CNOT gates do not introduce tunable parameters, they play a crucial role in enabling the entanglements between the qubits to increase possible interactions in the circuit. An alternate form of Generic Ansatz without the last CNOT (shown in Fig. 3.3) was used to test the relationship between the ansatz structure and the problem Hamiltonian of similar form. It is assumed that the more similar the ansatz circuit is to the problem structure, the better the result of the optimization.

Although Fig. 3.2 depicts the circuit for four qubits, the design is scalable and was implemented for up to twelve qubits in this work. This ansatz stands out for its simplicity; as only a single layer of tunable R_y gates followed by non-tunable CNOT gates work hand in hand to reach the desired convergence.

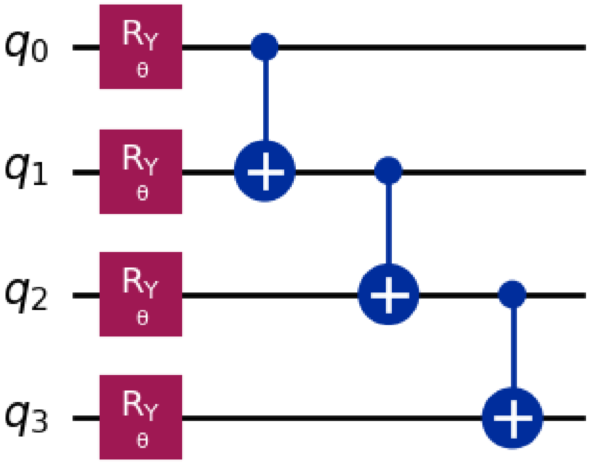
q_0
q_1
q_2
q_3
R_Y
θ

FIGURE 3.3: Generic Ansatz: Y-rotation gates followed by a chain CNOT gates with no CNOT connecting the end qubits.

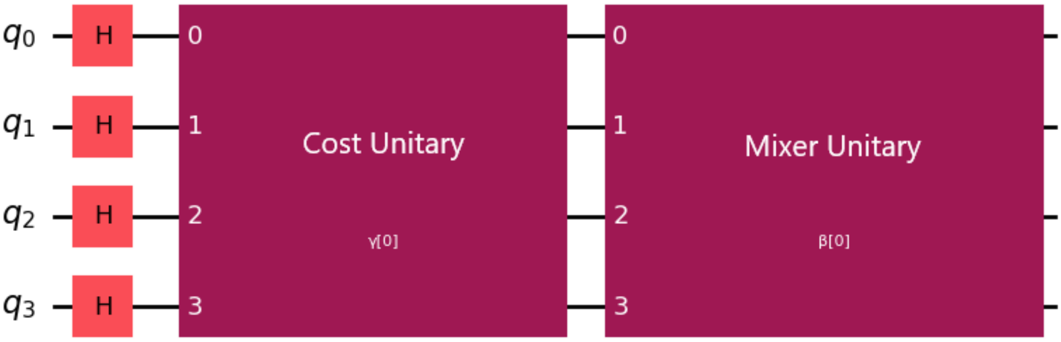
q_0
q_1
q_2
q_3
H
0
1
2
3
Cost Unitary
γ[0]
Mixer Unitary
β[0]

FIGURE 3.4: QAOA Ansatz: A layer of Hadamard gates followed by a layer of Cost Unitary and a layer of Mixer Unitary

3.2.2 QAOA Ansatz

The Fig. 3.4 shows the ansatz introduced by Farhi, Goldstone, and Gutmann, 2014 in their paper on the Quantum Approximation Optimization Algorithm. This hybrid algorithm was presented to approximately solve combinatorial optimization problems using near-term quantum devices. The ansatz circuit for this algorithm (sometimes also called Quantum Alternating Operator Ansatz with the same acronym) consists of alternating layers of parameterized unitaries corresponding to the cost Hamiltonian H_C and a mixer Hamiltonian H_M. Instead of a single parameter as seen in the Generic Ansatz, it consists of unique parameters for both layers represented by γ and β. The cost Hamiltonian circuit $U(H_C, \gamma) = e^{-i\gamma H_C}$ encodes the optimization objective of the problem, like in the case of the MaxCut problem, H_C is defined as $-\sum_{(i,j)\in E} \sigma_z^i \sigma_z^j$. This means that the first unitary layer has the $ZZ(\gamma)$ interaction between the qubits. The second unitary, the mixer Hamiltonian layer $U(H_M, \beta) = e^{-i\beta H_M}$, consists of R_x gates to assist in the exploration of the solution space.

The parameter p is a key hyperparameter in the QAOA ansatz that denotes the number of layers of the alternating unitaries. According to Wurtz and Love, 2022, increasing p improves the precision of the process, such that $p \to \infty$ ensures convergence to the exact ground state of the problem, albeit at the cost of greater circuit depth and computational resources.

The ansatz begins with an initial set of Hadamard gates to represent all the solutions states with equal probability in the form of the superposition state $|+\rangle^{\otimes n}$, followed by the cost and mixer Hamiltonians, classically optimizing the parameters to minimize the objective function.

To generate the QAOA ansatz, a graph is given as input which connects the circuit of the Cost Unitary part of the ansatz corresponding to the structure of that graph. Since the entanglement between the qubits depends on the shape of the input graph; to achieve the maximum entanglement in the Cost layer, complete graphs were used, like the one shown in Fig. 3.1, to generate the QAOA ansatz.

Chapter 4

Results

This section presents the results obtained from applying the variational quantum algorithm in several configurations to different problems using both ansatz and keeping the optimizer consistent throughout the process. It is stated that the hardware and software specifications along with the code implementation are provided in Appendix A. Additionally, readers are advised that not all the optimization runs lead to a converged value and the range of the x-axes in the plots given below varies based on converged energy values; please interpret the plots accordingly. In this research, the performance of the Generic Ansatz and Quantum Alternating Operator Ansatz or QAOA ansatz was evaluated for solving the electronic structure problem of lithium hydride (LiH), the MaxCut combinatorial optimization problem, and approximating the ground state of the Transverse-Field Ising Model. For all comparisons, the hyperparameter p for the QAOA ansatz was set to 1, so the layers of ansatz are identical for comparison. At times, the correlation between the chosen ansatz and the problem Hamiltonian yields unexpected performance outcomes, highlighting the complex interplay between the ansatz structure and the problem characteristics. Although these results provide valuable insights into the effectiveness of each ansatz, certain limitations, like prolonged optimization times and comparability issues persist.

4.1 Ground State of LiH

To evaluate the performance of different variational ansätze in solving molecular electronic structure problems, the ground state energy of the lithium hydride (LiH) molecule was approximated using both the Generic Ansatz and the QAOA Ansatz. In both cases, the atomic coordinates of the molecule were kept the same, the lithium atom is placed at the origin $(0, 0, 0)$ and the hydrogen atom is positioned along the z-axis at $(0, 0, 1.5949)$, distance calculated in Å (angstroms). Along with that, the optimizer was also kept constant

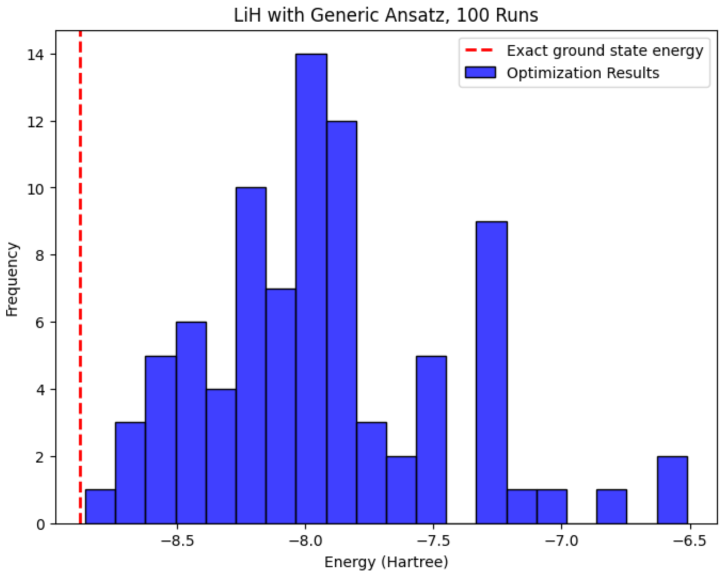

FIGURE 4.1: Convergence of the ground state energy of LiH molecule using the Generic Ansatz over 100 optimization runs with random initial parameters for each run. The red-dashed line represents the reference energy calculated using the NumPy exact solver.

as COBYLA in both configurations, and the number of layers for both ansätze was set to one.

To benchmark the accuracy of the results, the NumPy eigensolver diagonalizes the molecular Hamiltonian. The NumPy exact eigensolver scales exponentially with the size of the system because it relies on matrix diagonalization, which has a computational complexity of $\mathcal{O}(2^n \times 2^n)$, where n is the number of qubits. This means the memory required and the time taken to compute the eigenvalues grow exponentially with the number of qubits, making it impractical for larger systems. Although it doesn't scale well, it works fine for small systems and can provide a useful reference point for evaluating the algorithm's accuracy. The reference ground state energy of the LiH molecule, computed using the NumPy exact solver is:

$$E_g = -8.877783454702\,\text{Hartree}$$

Fig. 4.1 shows the frequency with which the parameter converged to each energy value compared to the reference ground state energy. The most frequently converged energy values are slightly deviated from the exact value, indicating the sensitivity of the VQAs to initial parameters. In this particular plot, the closest value to the exact energy is reached only once. Compared

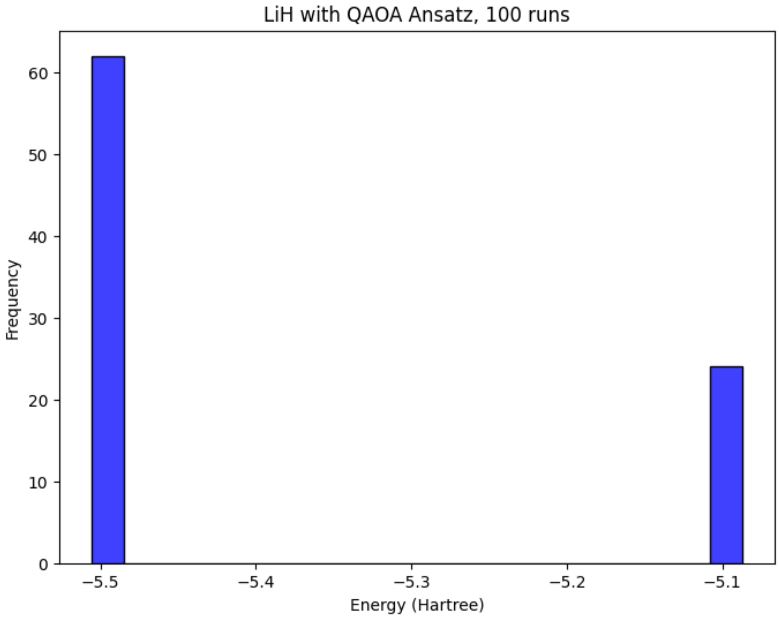

FIGURE 4.2: Convergence of the ground state energy of LiH molecule using the QAOA Ansatz over 100 optimization runs with random initial parameters for each run.

to Fig. 4.2, the converged energies show a more significant deviation from the reference point. Although, for a fair comparison, the layers of the ansätze were supposed to be set to one, increasing p for the QAOA Ansatz does not provide any better results. But the energies are not as spread out as in the case of Fig. 4.1, showing that the QAOA Ansatz optimization gets stuck in the local minima which do not let the parameter reach closer to the exact value. Interestingly, the total frequency of both configurations is almost identical, around 85 out of 100 optimization runs. This suggests that the optimization process is overall stable, but some initial values fail to lead to any convergence.

The results show that while the Generic Ansatz tends to produce a wider spread of energy values, suggesting greater sensitivity to the initial parameters, it generally brings the parameter closer to the exact ground state. In contrast, the QAOA Ansatz exhibited a bimodal convergence behavior, i.e., consistently falling into one of the two energy bins depending on the initial parameters. It suggests that the QAOA Ansatz approach gets stuck in the local minima and fails to reach closer to the exact value.

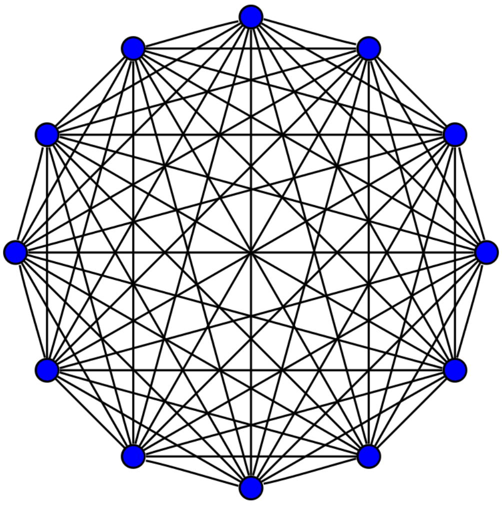

FIGURE 4.3: A complete graph of 12 nodes.

4.2 MaxCut Problem on a K-12 Graph

The MaxCut problem was solved on a complete graph of 12 nodes, where each node is connected to every other node as shown in Fig. 4.3. The task was to maximize the number of edges cut between two sets of nodes. The correct solution for the MaxCut problem on a K-12 graph is known to be 36, representing the maximum possible number of edges that can be cut. To obtain the lowest energy of the MaxCut Hamiltonian, 36 edges cut correspond to an energy of -36 units. Both the Generic Ansatz and the QAOA Ansatz were employed to solve this problem. And both configurations resulted in bimodal convergence, similar to the behavior seen in the LiH ground state optimization using the QAOA Ansatz. In the case of Generic Ansatz, the optimization showed impressive results, with around 98 of the 100 results converging to the correct energy value and two of the converged values landing slightly off, as shown in Fig. 4.4. This demonstrates that the Generic Ansatz consistently found optimal solutions with a high degree of accuracy.

On the other hand, the QAOA Ansatz, which is specifically designed for combinatorial problems, showed slightly worse accuracy. Even the worst result from the Generic Ansatz was slightly better than the best result from the QAOA Ansatz. This discrepancy can be attributed to the choice of the hyperparameter $p = 1$ for the QAOA Ansatz, which likely limited its expressiveness. The QAOA Ansatz also exhibited bimodal convergence but with a lower proportion of successful convergences. Specifically, around 68 runs converged near the correct energy, while 26 of them did not reach the correct

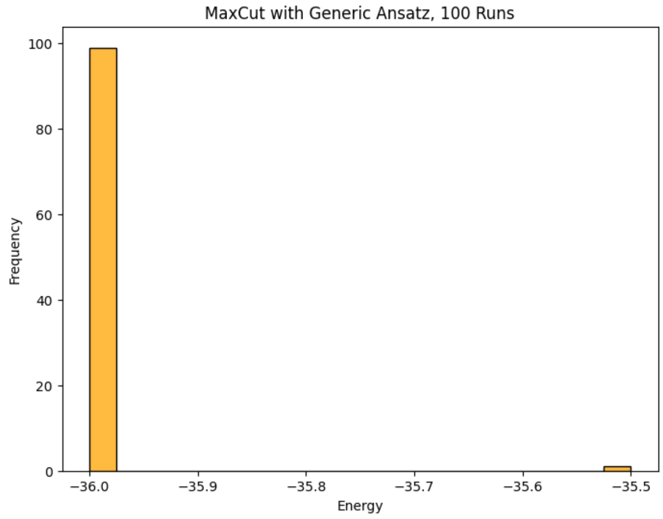

FIGURE 4.4: Optimization results for the MaxCut problem on a complete graph of 12 vertices (K-12) using the Generic Ansatz.

value, and others did not converge at all.

Overall, both ansätze demonstrated strong performance in solving the given problem, but the Generic Ansatz performed slightly better as it converged closer and more frequently to the right result with almost no failed optimizations.

4.3 Solving the Transverse-Field Ising Model

The Transverse-Field Ising Model (TFIM), as discussed in Ch. 3, was solved using the Generic Ansatz and the QAOA Ansatz to evaluate their performance regarding a quantum spins system consisting of 12 spins. Two forms of this model were considered: one was structured as a chain of interacting spins, with each spin coupled to its nearest neighbors and subjected to a transverse magnetic field. The other had the same properties except that the last spin was also connected to the first spin, forming a circular spin configuration. The exact ground state energies for these two systems, represented by E_{chain} and E_{circ}, were also calculated by diagonalizing the respective Hamiltonian matrices. In this work, the transverse field strength is used as a scaling factor, as $g = 0.8$, so, all the energy values are expressed in dimensionless units. Notably, all the results for this section also demonstrated bimodal convergence behavior. The exact values are as follows:

$$E_{\text{chain}} = -13.391526827970027$$

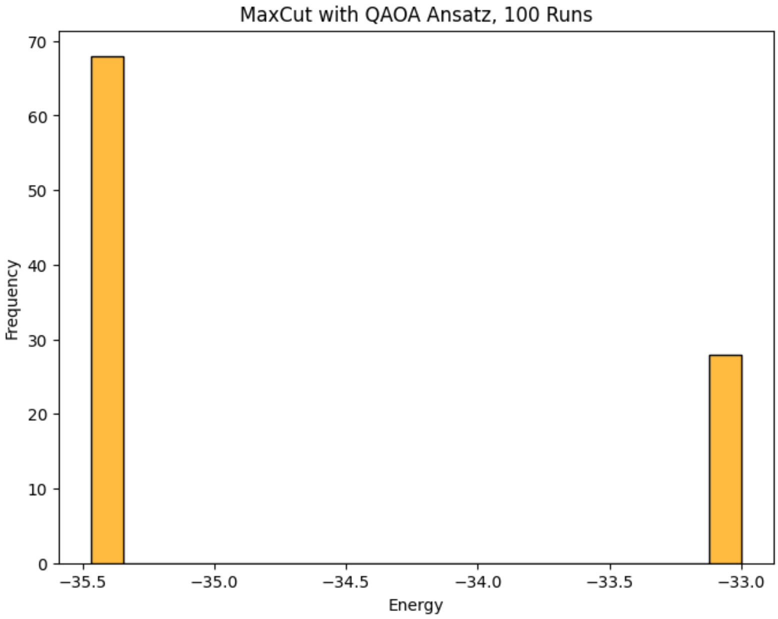

FIGURE 4.5: Optimization results for the MaxCut problem on a K-12 graph using the QAOA Ansatz.

$$E_{\text{circ}} = -14.021144494312773$$

In a straight chain of spins, the structure of the problem is similar to the Generic Ansatz but without the CNOT connecting the last qubit to the first, making it essentially a chain of CNOTs. This setup of the VQA was expected to demonstrate better results than the TFIM chain with the unaltered Generic Ansatz. The results for both of these configurations are shown in Fig. 4.6 and Fig. 4.7. While the change in converged energies is not drastic from the unaltered Generic Ansatz setup, it can be seen that the assumption about the similar structure leading to more accurate results in this particular case is holding. Additionally, Fig. 4.7 shows comparable number of convergences to Fig. 4.6, specifically, around 50 and 58 respectively out of 100 runs, the rest of the runs did not converge to any value.

Now considering the circular configuration of the Transverse-Field Ising Model, where there is a connection between the last and the first spin. Again, it was presumed that the circular model with the unaltered Generic Ansatz which comprises CNOTs in the same pattern would lead to better results, but both plots in Fig. 4.8 and Fig. 4.9 show almost identical results. The number of successful convergences is slightly higher for the unaltered ansatz with around 75 successful convergences to 68 for the other case.

The QAOA Ansatz was also evaluated for both configurations of the Transverse Field Ising Model with the hyperparameter of the ansatz set to $p = 1$.

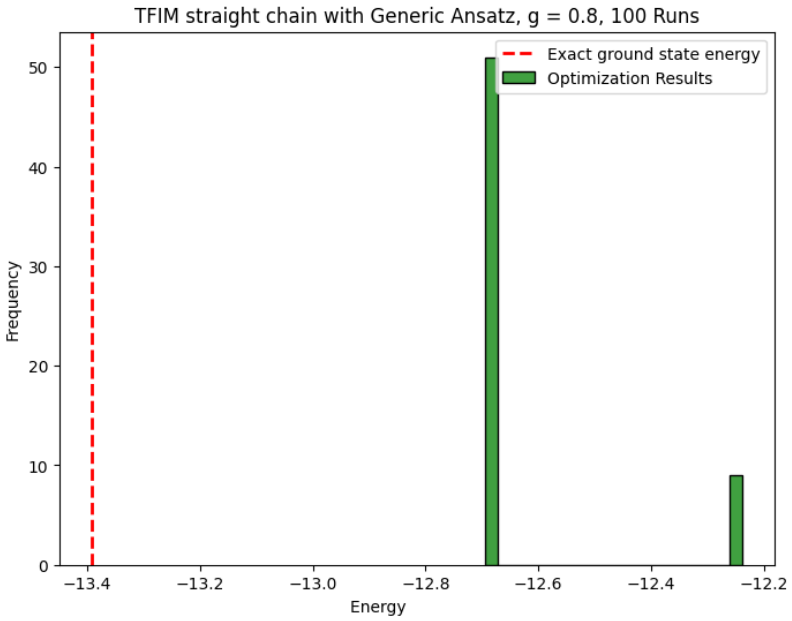

FIGURE 4.6: Optimization results for the TFIM chain using Generic Ansatz over 100 runs using the transverse field strength $g = 0.8$. The red dashed line shows the exact ground state energy for comparison.

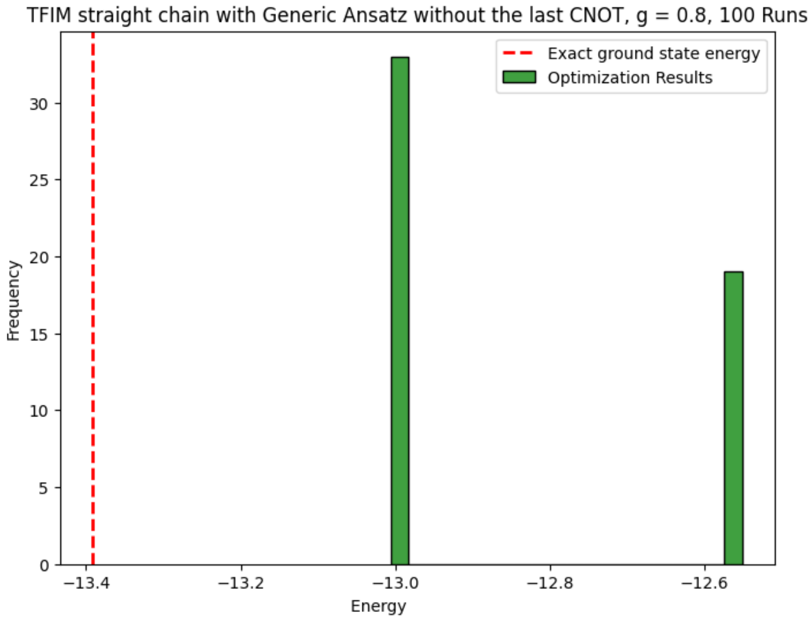

FIGURE 4.7: Optimization results for the TFIM chain using Generic Ansatz without the last CNOT over 100 runs using the transverse field strength $g = 0.8$. The red dashed line shows the exact ground state energy for comparison.

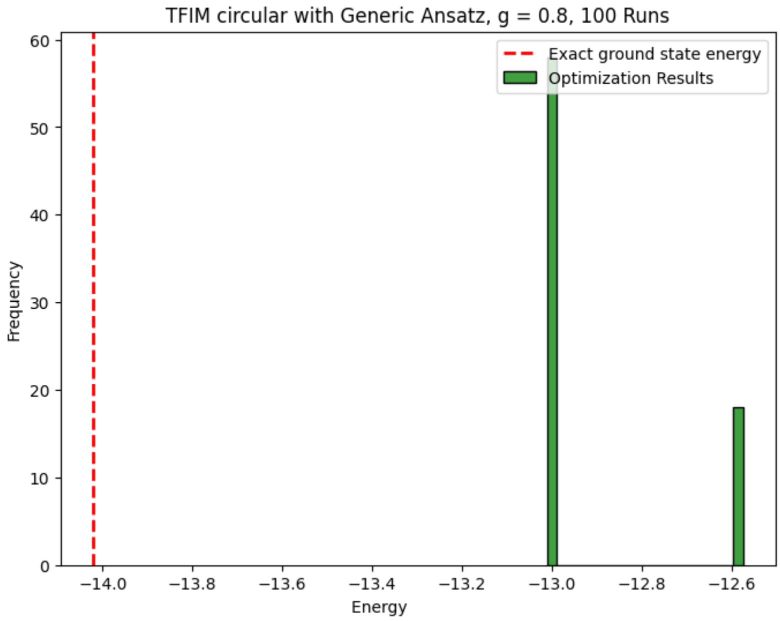

FIGURE 4.8: Optimization results for the circular TFIM using Generic Ansatz over 100 runs using the transverse field strength $g = 0.8$. The red dashed line shows the exact ground state energy for comparison.

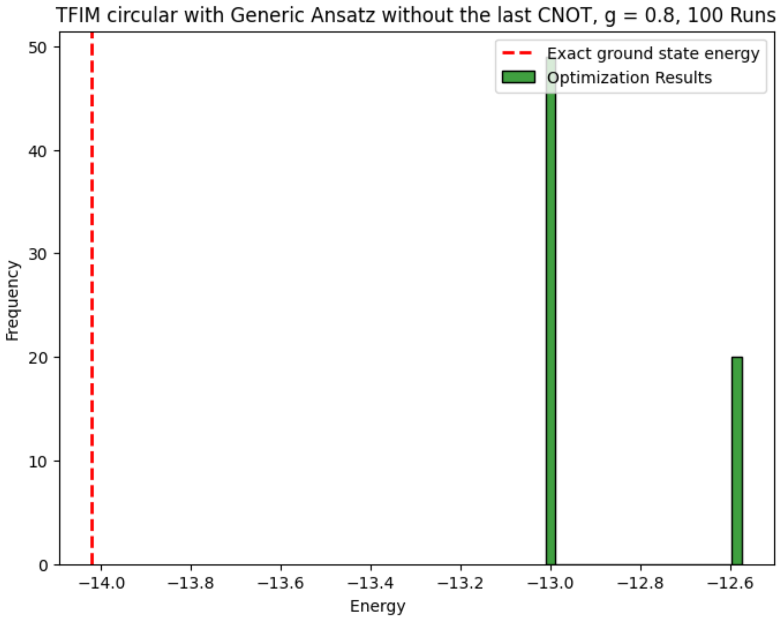

FIGURE 4.9: Optimization results for the circular TFIM using Generic Ansatz without the last CNOT over 100 runs using the transverse field strength $g = 0.8$. The red dashed line shows the exact ground state energy for comparison.

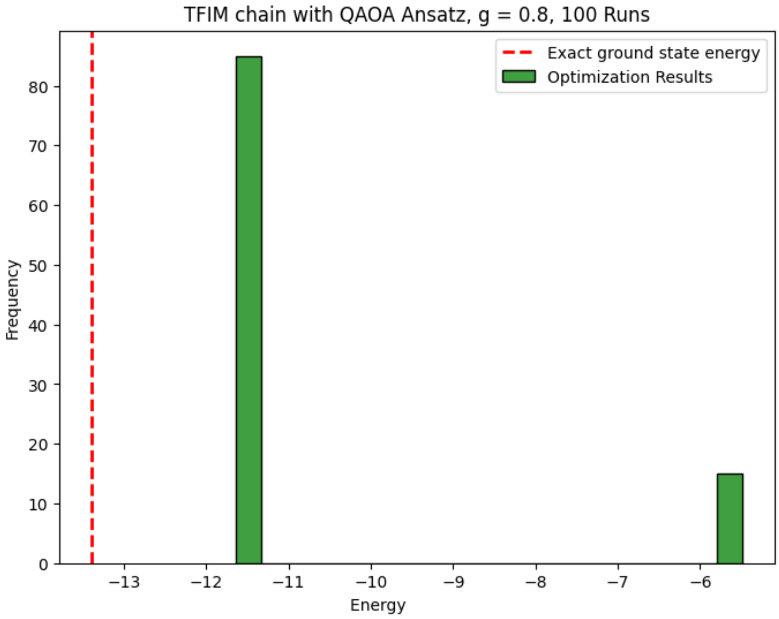

FIGURE 4.10: Optimization results for the TFIM chain using QAOA Ansatz over 100 runs using the transverse field strength $g = 0.8$. The red dashed line shows the exact ground state energy for comparison.

The results suggest that the QAOA Ansatz correlated to a similar degree with both of the cases of TFIM, as shown in Fig. 4.10 and Fig. 4.11. It is to be noted that the occurrences of reaching a final optimization value were similar in both cases as well, but impressively higher than all of the convergences using the Generic Ansatz. On the other hand, the optimization using QAOA Ansatz could not reach as close to the exact ground state energy as did the parameters for the Generic Ansatz. The least accurate result of any case using the Generic Ansatz remained closer to the reference energy than the most precise value obtained using the QAOA ansatz.

In summary, the comparative analysis of the Generic Ansatz and the QAOA Ansatz across the LiH ground state energy estimation, the MaxCut problem on a complete graph, and the Transverse-Field Ising Model has highlighted the nuanced relationship between the ansatz structure and problem type. One possible reason for this could be that the Generic Ansatz can explore a larger parameter space, allowing it to capture more correlations of the target Hamiltonians compared to the QAOA Ansatz. The Generic Ansatz generally exhibited stronger performance, converging more frequently and closely to the exact solution in all three problem scenarios compared to the QAOA Ansatz. Although we can attribute these limitations shown by the

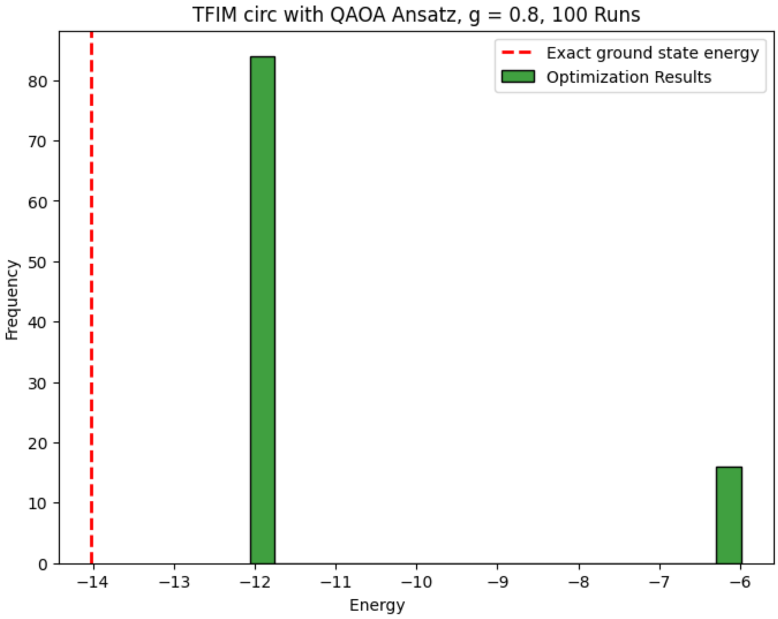

FIGURE 4.11: Optimization results for the circular TFIM using QAOA Ansatz over 100 runs using the transverse field strength $g = 0.8$. The red dashed line shows the exact ground state energy for comparison.

QAOA Ansatz to the number of layers we used, it should also be noted that only one layer of the Generic Ansatz was used throughout the process. The most unexpected result was the superior performance of the Generic Ansatz when it came to the MaxCut problem, whereas the QAOA Ansatz, despite being specifically designed for combinatorial optimization tasks, deviated a bit from the correct solution. This gap between the two ansätze in this particular problem can be closed by increasing the number of layers for the QAOA Ansatz, but that also increases the computational time. And the Generic Ansatz can accomplish the same task faster with one layer. The Generic Ansatz when used without the last connecting CNOT with the chain of spins in TFIM showed promising results. However, the Generic Ansatz against circular TFIM did not provide any benefit. Another point to note was the bimodal convergence behavior captured several times during the process. Overall, the Generic Ansatz demonstrated more adaptability to various problem types, consistently yielding solutions closer to the optimal values than the QAOA Ansatz.

Chapter 5

Conclusion & Outlook

This thesis explored the relationship between the ansatz design and the specific objective functions within the framework of the Variational Quantum Algorithms. By comparing the performance of the Generic Ansatz and the Quantum Alternating Operator Ansatz (QAOA Ansatz), this study assessed their effectiveness in approximating the ground state energies of some target Hamiltonians. Three distinct problems were considered for this analysis: the electronic structure of lithium hydride (LiH), the MaxCut combinatorial optimization problem, and the Transverse-Field Ising Model (TFIM). Each ansatz was examined for each problem from the set, as well as additional cases of TFIM and Generic Ansatz were researched for this work.

The comparative analysis of the Generic Ansatz and the QAOA Ansatz highlighted their varying strengths and weaknesses when applied across various problem types. The Generic Ansatz demonstrated stronger performance, converging more frequently and closely to the exact solution in all three problem scenarios as compared to the QAOA Ansatz. Although there were more convergences when the QAOA Ansatz was applied to TFIM, the accuracy of the expectation values was worse than that of the Generic Ansatz with TFIM. This performance gap can be attributed to the hyperparameter for the QAOA Ansatz being $p = 1$, but the number of layers for both ansätze was set to one for fairer comparison. The argument to not choose the QAOA Ansatz with larger number layers is the computational overhead, since the Generic Ansatz is exhibiting better results with one layer. But it is to be noted that it was assumed that a maximally connected circuit for the Cost Unitary of the QAOA leads to a better result, so complete graphs are used to generate the Cost Unitary for this ansatz.

The Generic Ansatz, altered to the form without the last CNOT and applied to the TFIM chain of spins led to better results than the the general implementation of the Generic Ansatz with the TFIM chain. On the other hand, it did not offer any advantage when Generic Ansatz (which is circular in nature) was applied to the circular configuration of the TFIM. Another significant observation was the bimodal convergence behavior which was frequently captured throughout the optimization process. Overall, the Generic Ansatz showed greater adaptability to various problem types, consistently reaching the convergence closer to the optimal solution than the QAOA Ansatz.

A consistent use of COBYLA optimizer throughout the study was a deliberate choice to isolate the impact of ansatz design. While this approach provided a controlled comparison, it also constrained the exploration of how different classical optimizers might affect convergence behavior. This limitation suggests a promising direction for future research to explore the interaction between the ansatz design and classical methods.

Future research could expand on this analysis by incorporating more problem-specific ansätze and varying classical optimizers to evaluate their combined effects on algorithm performance. The scalability of the Generic Ansatz could also be tested with more complex molecules, harder combinatorial problems, and bigger spin models. Keeping the number of parameters consistent for the comparison of these ansätze is a task that can be explored further as well. It could also be plausible to test whether the Generic Ansatz performs as well as it did in simulation as compared to the QAOA Ansatz on the actual quantum hardware.

In conclusion, this thesis highlights the pivotal role of ansatz design in the Variational Algorithms workflow, describing how effectively different ansätze works perform across various problem Hamiltonians. It also seeks to offer insights that can inform the design of more effective quantum algorithms for a wide range of problems by incorporating the findings about the ansätze.

Appendix A

Supplementary Material

A.1 Software, Libraries and System Specs

The thesis was conducted using the following hardware and software configurations:

A.1.1 Hardware

- Device: MacBook Pro
- Processor: 3.1 GHz Dual-Core Intel Core i5
- Graphics: Intel Iris Plus Graphics 650 (1536 MB)
- Memory: 16 GB 2133 MHz LPDDR3 RAM

A.1.2 Software

- Programming language: Python 3.12.3 (Python, 2024)
- Quantum computing framework: Qiskit 1.0 (Qiskit, 2024)
- Optimization library: `scipy.optimize.minimize` with `method = 'COBYLA'` (Virtanen, Gommers, Oliphant, et al., 2020)
- Visualization tools: Matplotlib (Hunter, 2007), Seaborn (Waskom, 2021)
- Graph construction tool: NetworkX (Hagberg, Schult, and Swart, 2008)

A.2 Code Implementation

The source code used for the experiments and analyses in this thesis is available on GitHub at this link. The code includes all the implementations for the solutions of the problems discussed above and the scripts to perform the optimization runs and plot the results.

Bibliography

Arute, Frank, Kunal Arya, Ryan Babbush, et al. (2019). "Quantum supremacy using a programmable superconducting processor". In: *Nature* 574, pp. 505–510. DOI: `10.1038/s41586-019-1666-5`. URL: `https://doi.org/10.1038/s41586-019-1666-5`.

Bittel, Lennart and Martin Kliesch (Sept. 2021). "Training Variational Quantum Algorithms Is NP-Hard". In: *Physical Review Letters* 127.12. ISSN: 1079-7114. DOI: `10.1103/physrevlett.127.120502`. URL: `http://dx.doi.org/10.1103/PhysRevLett.127.120502`.

Born, Max and J. Robert Oppenheimer (1927). "Zur Quantentheorie der Molekeln [On the Quantum Theory of Molecules]". German. In: *Annalen der Physik* 389.20, pp. 457–484. DOI: `10.1002/andp.19273892002`.

Cao, Yudong et al. (2019). "Quantum Chemistry in the Age of Quantum Computing". In: *Chemical Reviews* 119.19. PMID: 31469277, pp. 10856–10915. DOI: `10.1021/acs.chemrev.8b00803`. eprint: `https://doi.org/10.1021/acs.chemrev.8b00803`. URL: `https://doi.org/10.1021/acs.chemrev.8b00803`.

Cerezo, M., A. Arrasmith, R. Babbush, et al. (2021). "Variational quantum algorithms". In: *Nature Reviews Physics* 3.9, pp. 625–644. DOI: `10.1038/s42254-021-00348-9`. URL: `https://doi.org/10.1038/s42254-021-00348-9`.

Farhi, Edward, Jeffrey Goldstone, and Sam Gutmann (2014). *A Quantum Approximate Optimization Algorithm*. arXiv: `1411.4028 [quant-ph]`. URL: `https://arxiv.org/abs/1411.4028`.

Fedorov, D.A., B. Peng, N. Govind, et al. (2022). "VQE method: a short survey and recent developments". In: *Mater Theory* 6.2, p. 2. DOI: `10.1186/s41313-021-00032-6`. URL: `https://doi.org/10.1186/s41313-021-00032-6`.

Fradkin, Eduardo (2013). *Field Theories of Condensed Matter Physics*. 2nd ed. Cambridge University Press.

Griffiths, David J. and Darrell F. Schroeter (2020). *Introduction to Quantum Mechanics*. 3rd. Cambridge University Press, p. 418. ISBN: 9781107189638.

URL: https://www.cambridge.org/core/books/introduction-to-quantum-mechanics/1C797EF35428F4D6AA61FF8F901DF789.

Hagberg, Aric A., Daniel A. Schult, and Pieter J. Swart (2008). "Exploring Network Structure, Dynamics, and Function using NetworkX". In: *Proceedings of the 7th Python in Science Conference (SciPy2008)*, pp. 11–15. URL: https://networkx.org.

Hunter, John D. (2007). "Matplotlib: A 2D Graphics Environment". In: *Computing in Science & Engineering* 9.3, pp. 90–95. DOI: 10.1109/MCSE.2007.55.

McClean, Jarrod R. et al. (Nov. 2018). "Barren plateaus in quantum neural network training landscapes". In: *Nature Communications* 9.1, p. 4812. DOI: 10.1038/s41467-018-07090-4. URL: https://doi.org/10.1038/s41467-018-07090-4.

PennyLane (2024). *BasicEntanglerLayers*. Accessed: December 18, 2024. URL: https://docs.pennylane.ai/en/stable/code/api/pennylane.BasicEntanglerLayers.html.

Peruzzo, A., J. McClean, P. Shadbolt, et al. (2014). "A variational eigenvalue solver on a photonic quantum processor". In: *Nat Commun* 5, p. 4213. DOI: 10.1038/ncomms5213. URL: https://doi.org/10.1038/ncomms5213.

Preskill, John (Aug. 2018). "Quantum Computing in the NISQ era and beyond". In: *Quantum* 2, p. 79. ISSN: 2521-327X. DOI: 10.22331/q-2018-08-06-79. URL: http://dx.doi.org/10.22331/q-2018-08-06-79.

Python (2024). *Python 3.12.3 Documentation*. Accessed: 2025-01-17. URL: https://docs.python.org/3.12/.

Qiskit (2024). *Qiskit: An Open-source Framework for Quantum Computing*. https://qiskit.org. Version 1.0, Accessed: 2025-01-17.

Reiher, Markus et al. (2017). "Elucidating Reaction Mechanisms on Quantum Computers". In: *Proceedings of the National Academy of Sciences* 114.29, pp. 7555–7560. DOI: 10.1073/pnas.1619152114. URL: https://www.pnas.org/doi/10.1073/pnas.1619152114.

Shor, Peter W. (Oct. 1997). "Polynomial-Time Algorithms for Prime Factorization and Discrete Logarithms on a Quantum Computer". In: *SIAM Journal on Computing* 26.5, 1484–1509. ISSN: 1095-7111. DOI: 10.1137/s0097539795293172. URL: http://dx.doi.org/10.1137/S0097539795293172.

Shusen Liu, et al. (2022). *Combinatorial Optimization Tutorial: Max-Cut Problem*. https://github.com/PaddlePaddle/Quantum/blob/master/tutorials/combinatorial_optimization/MAXCUT_EN.ipynb. Accessed: December 25, 2024.

Tilly, Jules et al. (2022). "The Variational Quantum Eigensolver: A review of methods and best practices". In: *Physics Reports* 986. The Variational Quantum Eigensolver: a review of methods and best practices, pp. 1–128. ISSN: 0370-1573. DOI: `https://doi.org/10.1016/j.physrep.2022.08.003`. URL: `https://www.sciencedirect.com/science/article/pii/S0370157322003118`.

Virtanen, Pauli, Ralf Gommers, Travis E. Oliphant, et al. (2020). "SciPy 1.0: Fundamental Algorithms for Scientific Computing in Python". In: *Nature Methods* 17, pp. 261–272. DOI: `10.1038/s41592-019-0686-2`.

Wang, Zhihui et al. (2018). "Quantum approximate optimization algorithm for MaxCut: A fermionic view". In: *Phys. Rev. A* 97 (2), p. 022304. DOI: `10.1103/PhysRevA.97.022304`. URL: `https://link.aps.org/doi/10.1103/PhysRevA.97.022304`.

Waskom, Michael L. (2021). "Seaborn: Statistical Data Visualization". In: *Journal of Open Source Software* 6.60, p. 3021. DOI: `10.21105/joss.03021`.

Wurtz, Jonathan and Peter J. Love (Jan. 2022). "Counterdiabaticity and the quantum approximate optimization algorithm". In: *Quantum* 6, p. 635. ISSN: 2521-327X. DOI: `10.22331/q-2022-01-27-635`. URL: `http://dx.doi.org/10.22331/q-2022-01-27-635`.